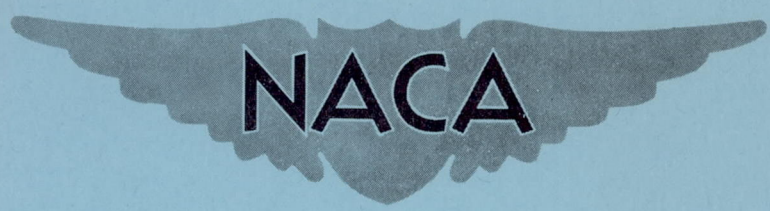


FILE COPY
NO /

★ CASE FILE
COPY

RM L51F01

NACA RM L51F01



RESEARCH MEMORANDUM

COMPARISON OF AIRFOIL SECTIONS ON TWO TRIANGULAR-
WING-FUSELAGE CONFIGURATIONS AT TRANSONIC SPEEDS
FROM TESTS BY THE NACA WING-FLOW METHOD

By Albert W. Hall and James M. McKay

Langley Aeronautical Laboratory
Langley Field, Va.

ON LOAN FROM THE FILES OF
NATIONAL ADVISORY COMMITTEE FOR AERONAUTICS
LANGLEY AERONAUTICAL LABORATORY
LANGLEY FIELD, HAMPTON, VIRGINIA

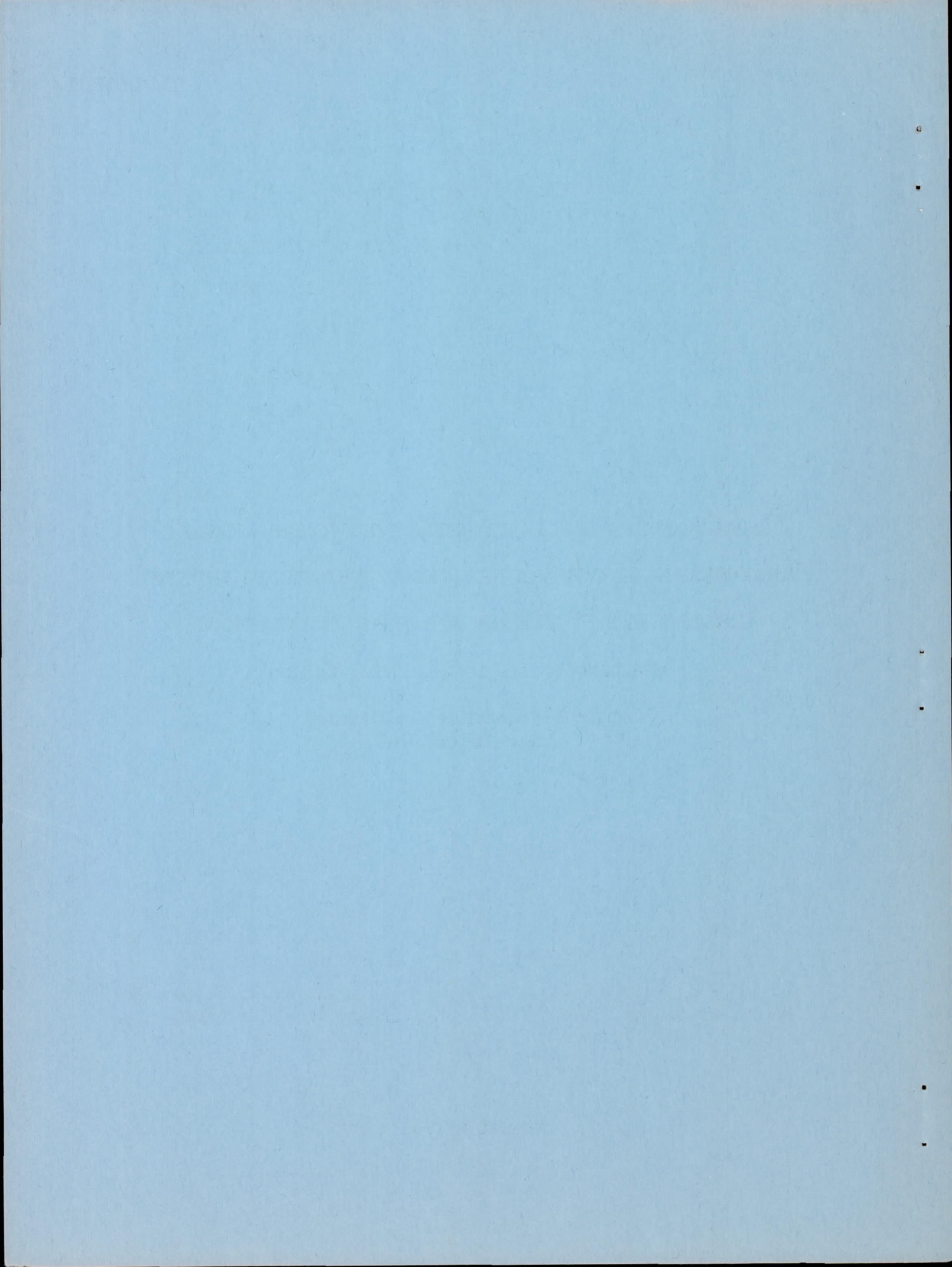
RETURN TO THE ABOVE ADDRESS.

REQUESTS FOR PUBLICATIONS SHOULD BE ADDRESSED
AS FOLLOWS:

NATIONAL ADVISORY COMMITTEE FOR AERONAUTICS
1512 H STREET, N. W.
WASHINGTON 25, D. C.

NATIONAL ADVISORY COMMITTEE FOR AERONAUTICS

WASHINGTON
August 8, 1951



NATIONAL ADVISORY COMMITTEE FOR AERONAUTICS

RESEARCH MEMORANDUM

COMPARISON OF AIRFOIL SECTIONS ON TWO TRIANGULAR-
WING-FUSELAGE CONFIGURATIONS AT TRANSONIC SPEEDS

FROM TESTS BY THE NACA WING-FLOW METHOD

By Albert W. Hall and James M. McKay

SUMMARY

Tests were made by the NACA wing-flow method at Mach numbers from 0.75 to 1.075 to determine the aerodynamic characteristics of four triangular-wing-fuselage models. Two models had wings of aspect ratio 2.31 (half-apex angle of 30°), one with an NACA 65-009 airfoil section and one with a 9-percent-thick biconvex section; the other two models had wings of aspect ratio 4.00 (half-apex angle of 45°), one with an NACA 65-006 airfoil section and one with a 6-percent-thick double-wedge section.

Measurements were made of normal force, chord force, and pitching moment for various angles of attack. The Reynolds number of the tests was approximately 1.5×10^6 based on the mean aerodynamic chord of the aspect-ratio-2.31 wing.

For the 9-percent-thick wings of aspect ratio 2.31, less favorable characteristics were indicated for the wing with the biconvex section than for the wing with the NACA 65-series section. The latter section gave generally greater lift-curve slopes, less drag rise with Mach number and with lift, and more rearward aerodynamic-center positions than the biconvex section. The variation of the lift and pitching moment with Mach number, moreover, was more gradual for the wing with the 65-series section and the drag-rise Mach number was slightly higher than that for the wing with the biconvex section.

Comparison of results for the double-wedge and 65-series sections on the thinner wings of aspect ratio 4.00 indicated similar trends although the differences were generally much smaller.

INTRODUCTION

As part of a program to determine the effect of leading-edge sweep and wing section and thickness on the aerodynamic characteristics of triangular wings at transonic and low supersonic speeds, several wing-fuselage configurations have been tested by the NACA wing-flow method.

The present paper is concerned primarily with the effect of wing section as indicated from results of tests of two 9-percent-thick wings of aspect ratio 2.31, one with an NACA 65-009 airfoil section and one with a biconvex section, and two 6-percent-thick wings of aspect ratio 4.00, one with an NACA 65-006 section and one with a symmetrical double-wedge section. Each wing was tested in combination with a slender fuselage and measurements were made of normal force, chord force, and pitching moment at various angles of attack through a Mach number range of 0.750 to 1.075.

SYMBOLS

M_L	local Mach number at surface of test section	
M	effective Mach number at wing of model	
q	effective dynamic pressure at wing of model, pounds per square foot	
R	Reynolds number based on mean aerodynamic chord of model	
e	half-apex angle of model wing, degrees	
α	angle of attack of model wing, degrees	
S	semispan-wing area of model, square feet	
b	span of model wing, inches	
c	local wing chord of model, inches	
\bar{c}	mean aerodynamic chord of model wing, inches	$\left(\frac{\int_0^{b/2} c^2 dy}{\int_0^{b/2} c dy} \right)$
y	spanwise coordinate, inches	

- L lift, pounds
- M pitching moment about 50-percent \bar{c} point, inch-pounds
- D drag, pounds
- C_L lift coefficient (L/qS)
- C_m pitching-moment coefficient ($M/qS\bar{c}$)
- C_D drag coefficient (D/qS)
- C_{D_0} drag coefficient at zero lift
- A aspect ratio ($4 \tan \epsilon$)
- $\frac{dC_L}{d\alpha}$ rate of change of lift coefficient with angle of attack
- $\frac{\Delta C_D}{\Delta C_L^2}$ average ratio of the increment of drag coefficient above the minimum to the square of the increment of lift measured from that corresponding to minimum drag coefficient
- $$\left[\frac{C_D - C_{D_{\min}}}{(C_L - C_L \text{ at } C_{D_{\min}})^2} \right]$$
- $\frac{dC_m}{dC_L}$ rate of change of pitching-moment coefficient with lift coefficient

APPARATUS AND TESTS

The tests were made by the NACA wing-flow method in which the model was mounted in a region of high-speed flow over the wing of a North American F-51D airplane.

The four semispan models tested consisted of four different triangular wings in combination with a fuselage. Two wings had an aspect ratio of 2.31 ($\epsilon = 30^\circ$), one with an NACA 65-009 section and one with a 9-percent-thick biconvex section; the other two wings had an aspect ratio of 4.00 ($\epsilon = 45^\circ$), one with an NACA 65-006 section and one with a 6-percent-thick double-wedge section (maximum thickness at $0.50\bar{c}$). The fuselage was a half-body of revolution of fineness ratio 12 and was fitted

with an end plate. The models were mounted about $1/64$ inch above the surface of the test section and fastened to a strain-gage balance below the test section by means of a shank which passed through a hole in the test section. The model and balance oscillated together thus allowing normal force, chord force, and pitching moment to be measured at various angles of attack. Details of the models are given in tables I and II and figures 1 and 2.

The chordwise distribution of local Mach number M_L along the airplane wing surface in the test region is shown in figure 3 for several values of airplane Mach number and lift coefficient. The local Mach number was determined from static-pressure measurements made with orifices flush with the surface in tests with the model removed. The vertical Mach number gradient was determined from measurements made with a static pressure tube located at various distances above the surface of the test section and found to be 0.009 per inch. The effective Mach number M at the wing of the model was determined as an average Mach number over the wing area of the model. A more detailed discussion of the determination of effective Mach number and effective dynamic pressure q can be found in reference 1.

The angle of attack was determined from measurements of model angle and local-flow angle. The local-flow angle was determined by a free-floating vane mounted outboard of the model station as discussed in reference 1.

The tests were made during high-speed dives of the F-51D airplane. Continuous measurements were made of angle of attack, normal force, chord force, and pitching moment of the model as the effective Mach number varied from 1.075 to 0.75 and as the model was oscillated through an angle-of-attack range of -3° to 10° . The Reynolds number range for the tests is shown in figure 4.

REDUCTION OF DATA

Lift, drag, and pitching-moment coefficients are based on the wing area extended to the fuselage center line as shown in figure 2. Pitching moments are referred to the 50-percent mean-aerodynamic-chord point.

Corrections have been made to the drag for the effect of buoyancy on the fuselage due to pressure gradients in the test region. Buoyancy effects on the wings were found to be negligible. No attempt has been made to correct the drag data for the effect of the fuselage end plate.

Figure 5 shows sample data for one oscillation through the angle-of-attack range. The Mach number varied from 0.88 to 0.86 during the

cycle. The curves faired through these points are used to give results for a Mach number of 0.87. Similarly, several cycles were reduced for each configuration and cross-plotted to show variations of the characteristics with Mach number at constant lift coefficients.

RESULTS AND DISCUSSION

Lift Characteristics

The variation of angle of attack α with Mach number M at constant lift coefficients C_L is shown in figure 6 for the four wing-fuselage configurations. The curves presented in figure 6(a) for the 9-percent-thick, $A = 2.31$ wings indicate a more gradual variation of α with M at constant values of C_L for the wing having the NACA 65-009 section than for the wing having the biconvex section. The curves presented in figure 6(b) for the 6-percent-thick, $A = 4.00$ wings indicate relatively little difference in the variation of α with M at constant values of C_L for the wing having the NACA 65-006 section and the wing having the double-wedge section.

The variation of the lift-curve slopes $dC_L/d\alpha$ with Mach number is presented in figure 7 for the four configurations. Also shown are calculated values obtained by the methods given in references 2 and 3. For both wing plan forms the values of $dC_L/d\alpha$ at $C_L = 0$ (fig. 7(a)) were higher throughout the Mach number range of the tests for the wings having NACA 65-series sections than for the wings having biconvex and double-wedge sections. The values of $dC_L/d\alpha$ at $C_L = 0.3$ (fig. 7(b)) indicate very little effect of section shape for either plan form at subsonic speeds but the same trend appears at higher speeds as was apparent at $C_L = 0$, that is, NACA 65-series sections produced higher lift.

The subsonic values of $dC_L/d\alpha$ calculated by the method of reference 2 are in closer agreement with the wings having 65-series sections than with the wings having the biconvex and double-wedge sections. At low-supersonic speeds the experimental values of $dC_L/d\alpha$ for each configuration are considerably lower than the values calculated by the method of reference 3.

The variation of $dC_L/d\alpha$ with M at $C_L = 0$ for other $A = 4.00$ wings is shown in references 4 and 5. The variation of $dC_L/d\alpha$ with M given in figure 7(a) for the wing with the NACA 65-006 section is similar to the curve presented in reference 4 for a wing with an

NACA 0005-63 section, particularly the sharp peak at $M = 0.95$. The values of $dC_L/d\alpha$ presented in reference 5 for a wing with an NACA 65A006 section are lower than the values given in figure 7(a) for a similar wing but are very close to the values given in figure 7(a) for the wing with the 6-percent-thick double-wedge section.

Drag Characteristics

The variation of drag coefficient C_D with M at constant values of C_L is shown in figure 8 for the four wing-fuselage configurations. The variation of drag coefficient at zero lift C_{D_0} with M for the configurations having 9-percent-thick, $A = 2.31$ wings (fig. 8(a)) indicates a lower drag over the Mach number range of the tests for the wing having the NACA 65-009 section than for the wing having the biconvex section. The differences indicated at subsonic speeds could be within the limitations of the test methods; however, the magnitude of the drag rise with Mach number is believed to be of the correct order and would indicate considerably less drag for the wing with the NACA 65-009 section than for the wing with the biconvex section at low-supersonic speeds. In the case of the two 6-percent-thick, $A = 4.00$ wings (fig. 8(b)) the differences in values of C_{D_0} are less than those of the two $A = 2.31$ wings but the same trend is evident, that is, the wing having the NACA 65-006 section gives lower drag over the Mach Number range of the tests than the wing having the double-wedge section, particularly at low-supersonic speeds. For both plan forms the drag-rise Mach number appears to be slightly higher for the wings having NACA 65-series sections.

The values of C_{D_0} for the $A = 4.00$ configuration with an NACA 65-006 airfoil section are lower than those given in reference 5 for a similar configuration (with a slightly different fuselage and without buoyancy corrections) but the magnitude of the drag rise is about the same in both cases.

The drag due to lift is represented by the factor $\Delta C_D/\Delta C_L^2$ and the variation of this factor with M is shown in figure 9 for the four wing-fuselage configurations. The values of $\Delta C_D/\Delta C_L^2$ are lower for the $A = 2.31$ wing with NACA 65-009 section than for the same plan form with biconvex section, whereas for the $A = 4.00$ wing there is very little difference indicated between values of $\Delta C_D/\Delta C_L^2$ for the NACA 65-006 and double-wedge sections. The reciprocal of the lift-curve slope (at $C_L = 0$) has also been plotted in figure 9 for each configuration and in each case the values of $\frac{1}{dC_L/d\alpha}$ are fairly close to the

corresponding values of $\Delta C_D / \Delta C_L^2$, indicating that the resultant-force increment due to angle of attack is acting nearly normal to the chord plane for all configurations.

Pitching-Moment Characteristics

The variation of pitching-moment coefficient C_m with M at constant values of C_L is shown in figure 10 for the four wing-fuselage configurations. For the 9-percent-thick, $A = 2.31$ wings the variation of C_m with M is more gradual for the wing having NACA 65-009 section than for the wing having the biconvex section. For the thinner, $A = 4.00$ wings the variation of C_m with M is quite similar for the NACA 65-006 and double-wedge sections.

The aerodynamic-center locations were determined from the slopes of the pitching-moment curves (dC_m/dC_L) at $C_L = 0$ and $C_L = 0.3$. (Sample pitching-moment curve for one configuration at $M = 0.87$ is shown in fig. 5.) The aerodynamic-center variation with M is shown in figure 11 for the four wing-fuselage configurations. For both plan forms where there is an appreciable difference in aerodynamic-center position it is farther forward for the wings having the biconvex or double-wedge sections than for the wings having the NACA 65-series sections.

CONCLUDING REMARKS

Tests made by the NACA wing-flow method on four triangular-wing-fuselage models, two having wings of aspect ratio 2.31, one with an NACA 65-009 section and one with a 9-percent-thick biconvex section and two having wings of aspect ratio 4.00, one with an NACA 65-006 section and one with a 6-percent-thick double-wedge section indicate these results at Mach numbers between 0.75 and 1.075.

For the 9-percent-thick wings of aspect ratio 2.31 less favorable characteristics were indicated for the wing with the biconvex section than for the wing with the NACA 65-series section. The latter section gave generally greater lift-curve slopes, less drag rise with Mach number and with lift, and more rearward aerodynamic-center positions than the biconvex section. The variation of the lift and pitching moment with Mach number, moreover, was more gradual for the wing with the 65-series section, and the drag-rise Mach number was slightly higher than for the wing with the biconvex section.

Comparison of results for the double-wedge and NACA 65-series sections on the thinner wings of aspect ratio 4 indicated similar trends, although the differences were generally much smaller.

Langley Aeronautical Laboratory
National Advisory Committee for Aeronautics
Langley Field, Va.

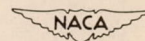
REFERENCES

1. Johnson, Harold I.: Measurements of Aerodynamic Characteristics of a 35° Sweptback NACA 65-009 Airfoil Model with $\frac{1}{4}$ -Chord Plain Flap by the NACA Wing-Flow Method. NACA RM L7F13, 1947.
2. DeYoung, John: Theoretical Additional Span Loading Characteristics of Wings with Arbitrary Sweep, Aspect Ratio, and Taper Ratio. NACA TN 1491, 1947.
3. Brown, Clinton E.: Theoretical Lift and Drag of Thin Triangular Wings at Supersonic Speeds. NACA Rep. 839, 1946. (Formerly NACA TN 1183.)
4. Heitmeyer, John C., and Stephenson, Jack D.: Lift, Drag, and Pitching Moment of Low-Aspect-Ratio Wings at Subsonic and Supersonic Speeds - Plane Triangular Wing of Aspect Ratio 4 with NACA 0005-63 Section. NACA RM A50K24, 1951.
5. Sleeman, William C., Jr., and Becht, Robert E.: Aerodynamic Characteristics of a Delta Wing with Leading Edge Swept Back 45° , Aspect Ratio 4, and NACA 65A006 Airfoil Section. Transonic-Bump Method. NACA RM L9G22a, 1949.

TABLE I

GEOMETRIC CHARACTERISTICS OF MODEL CONFIGURATIONS

<u>Wings:</u>				
Section	Biconvex	NACA 65-009	Double wedge	NACA 65-006
Thickness ratio, percent chord	9	9	6	6
Half-apex angle, degrees	30	30	45	45
\bar{c} , in.	4.07	4.07	3.02	3.02
Semispan area including projected area of wing in fuselage, sq in.	10.78	10.78	10.26	10.26
Aspect ratio	2.31	2.31	4.0	4.0
Dihedral, deg	0	0	0	0
Incidence, deg	0	0	0	0
<u>Fuselage:</u>				
Section	Modified 65-series body of revolution			
Length, in.	14.0			
Maximum diameter at 50 percent length, in.	1.17			
Fineness ratio	12.0			



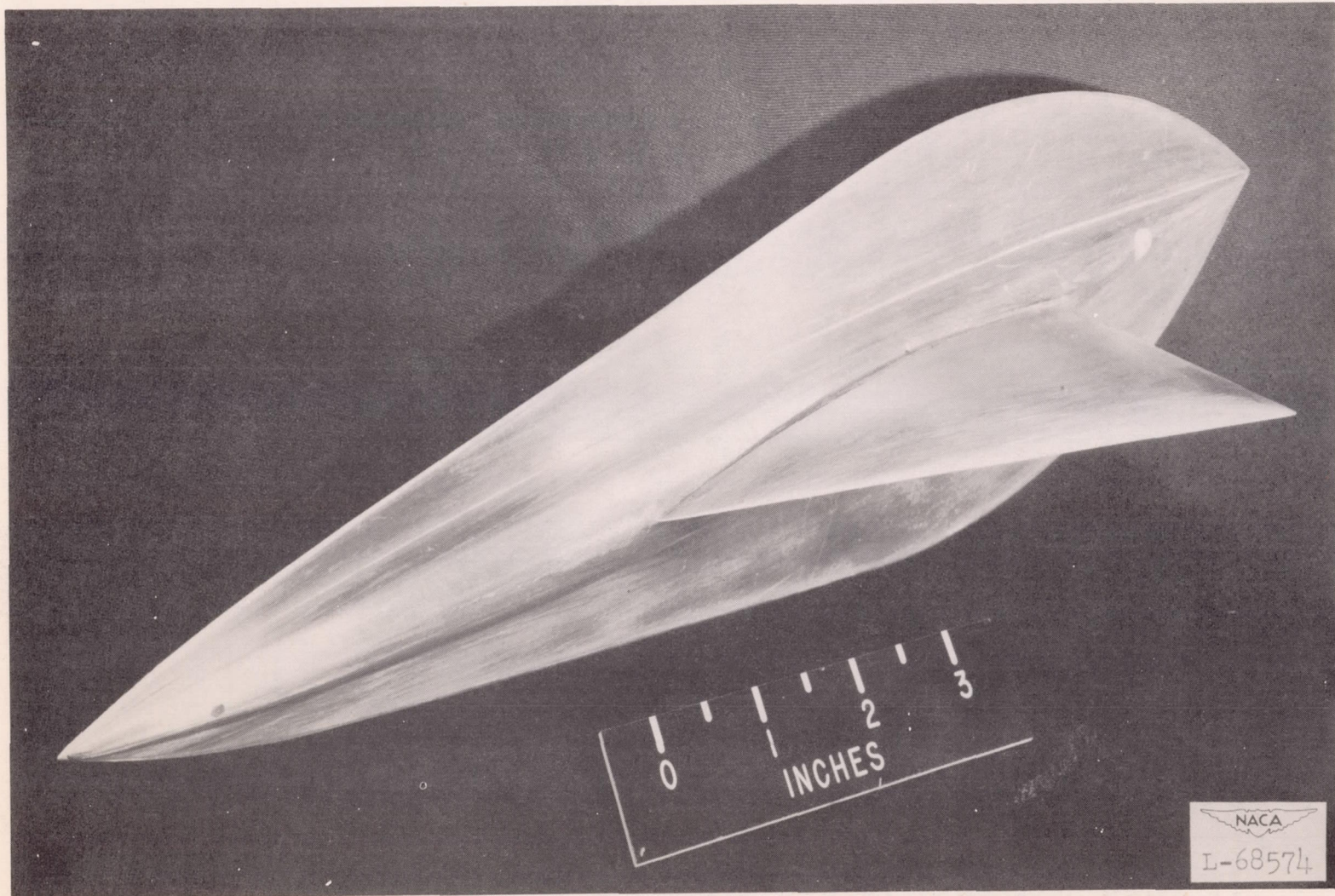


Figure 1.- Photograph of semispan wing-fuselage model and end plate.
Wing of $A = 2.31$, 9-percent-thick biconvex section.

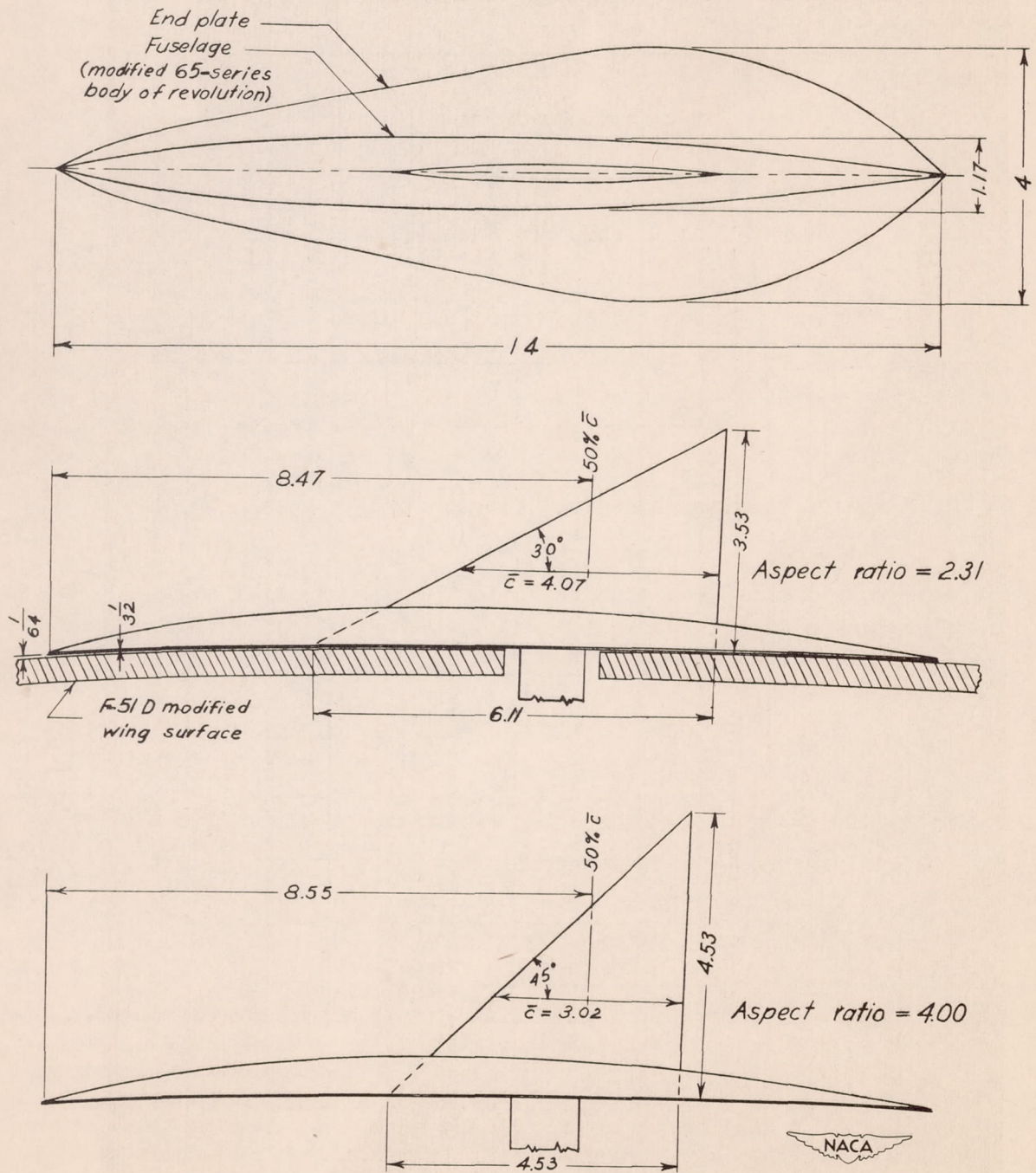


Figure 2.- Details of wing-fuselage models.

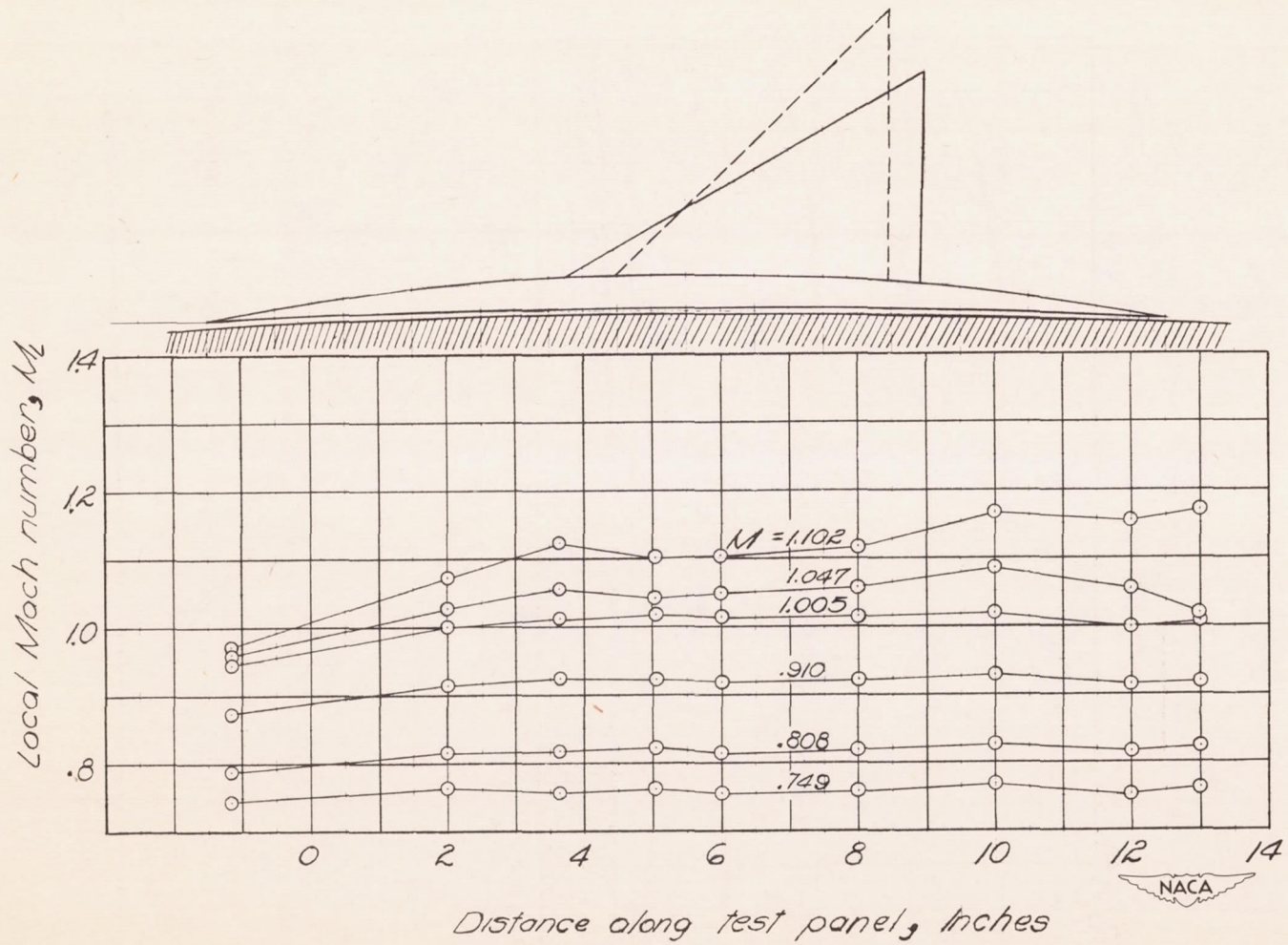


Figure 3.- Typical chordwise variation of Mach number in the test region on the surface of the airplane wing for several Mach numbers at the wing of the model. Chordwise location of model is also shown.

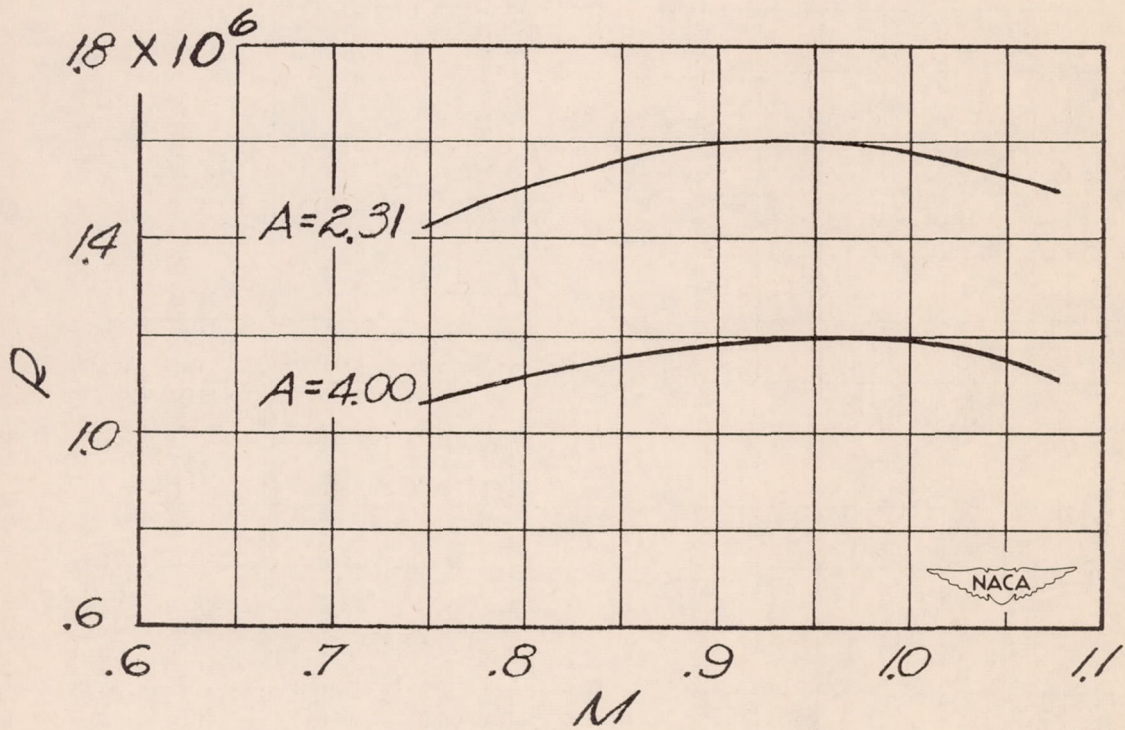
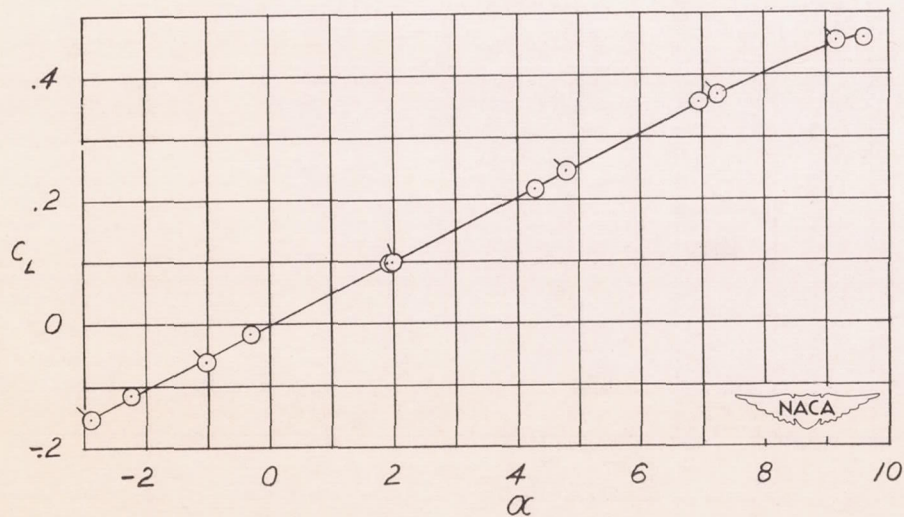
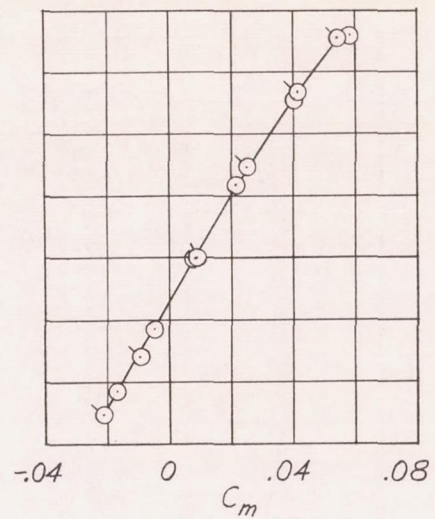
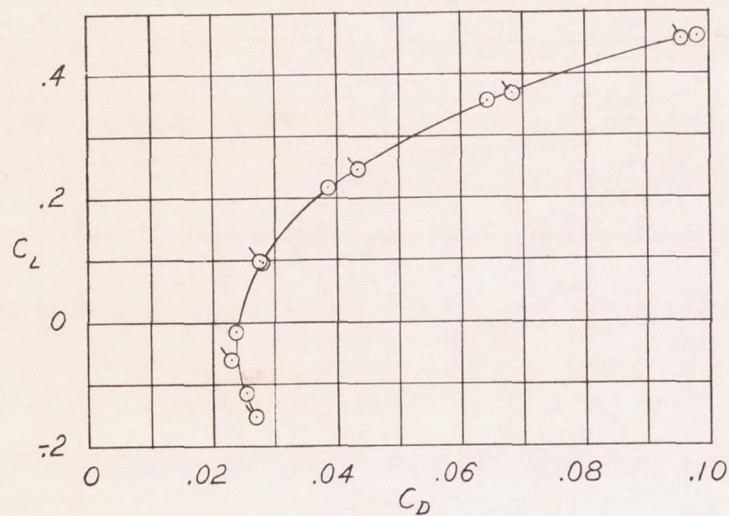


Figure 4.- Variation of test Reynolds number with effective Mach number.



○ increasing α
 ⊙ decreasing α

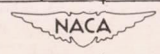
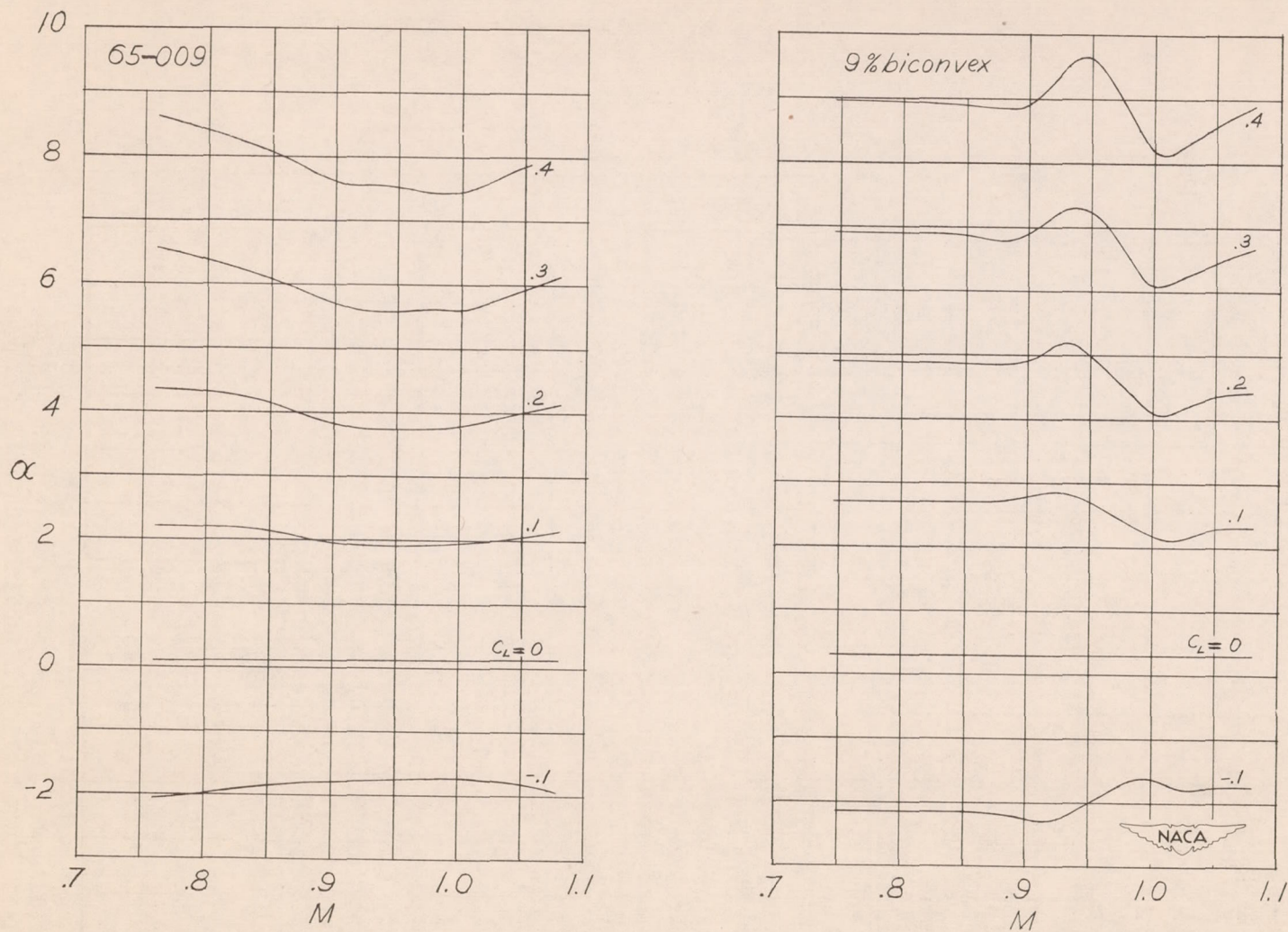
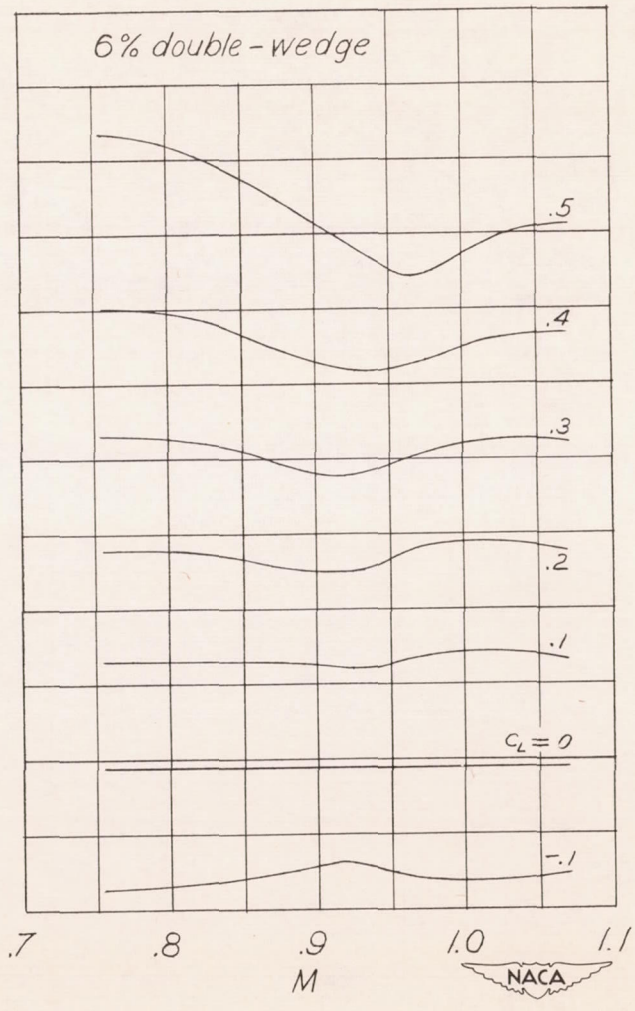
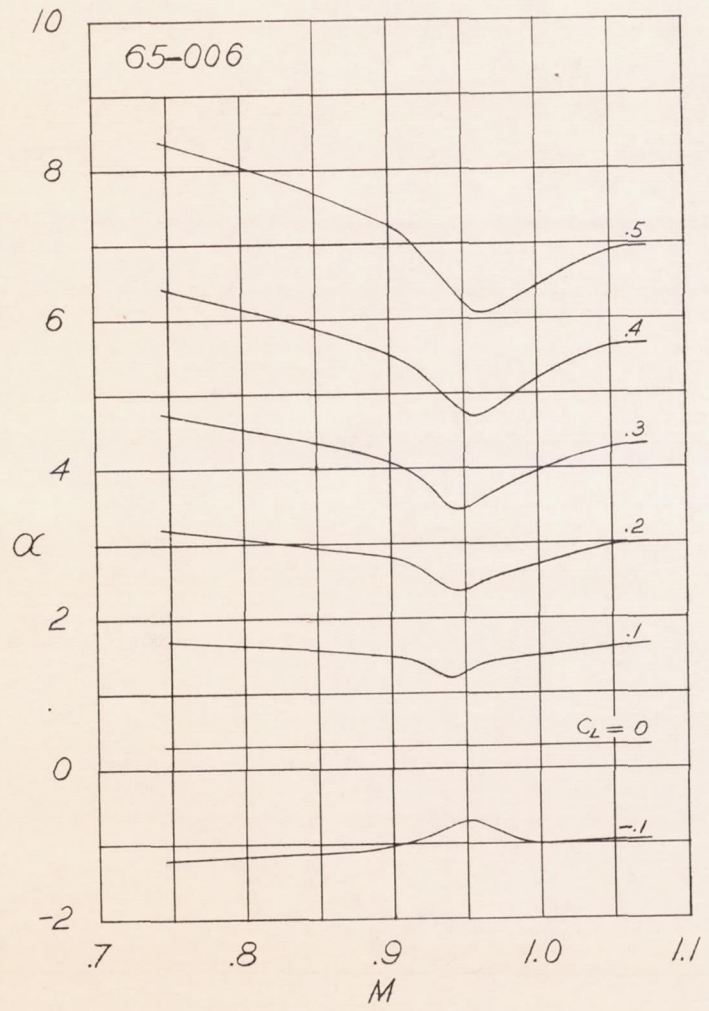


Figure 5.- Sample data for wing-fuselage model with $A = 2.31$ wing having NACA 65-009 section. $M = 0.87$.



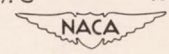
(a) Wing aspect ratio, 2.31.

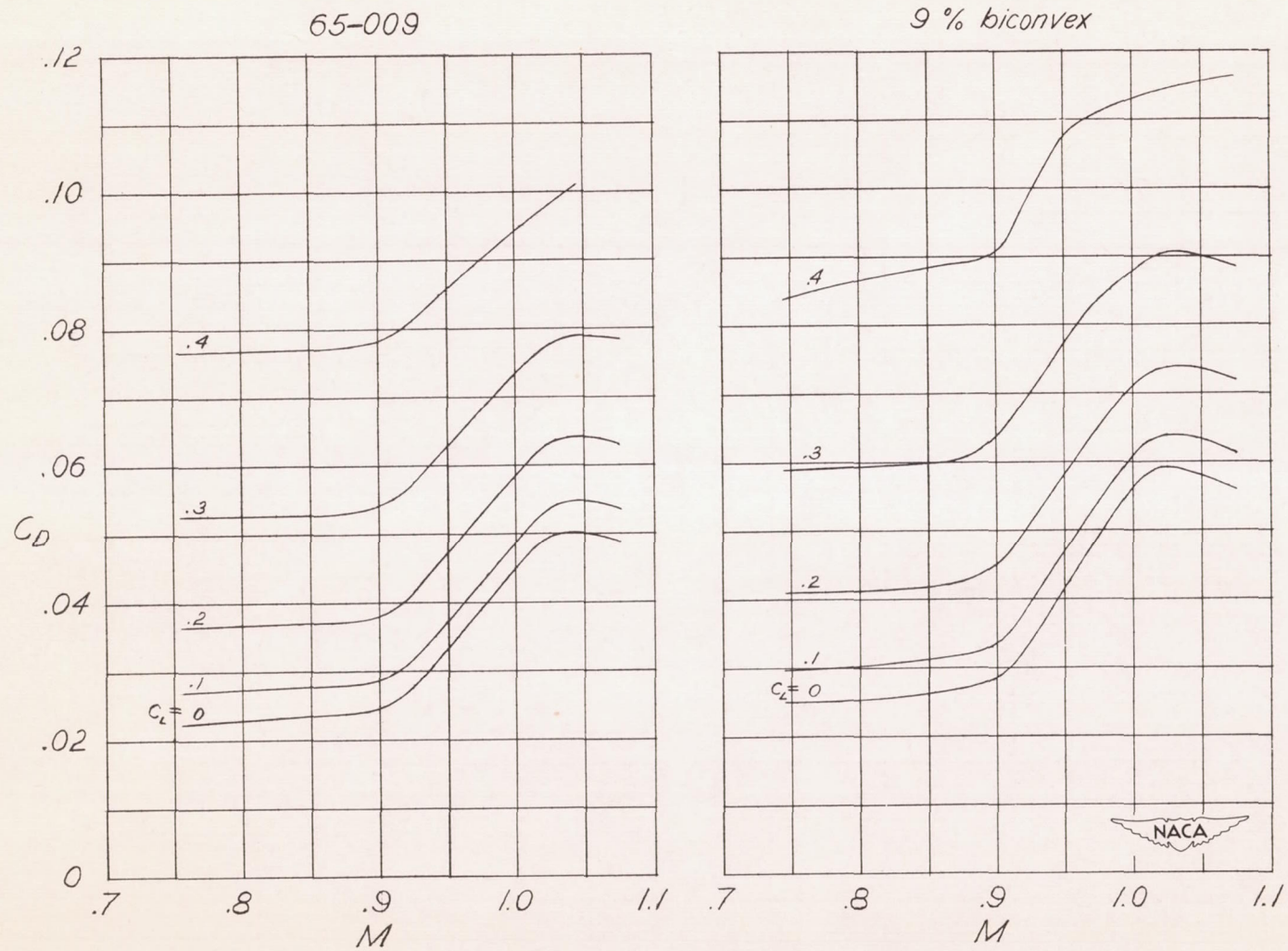
Figure 6.- Variation of angle of attack with Mach number at constant lift coefficient for wing-fuselage models.



(b) Wing aspect ratio, 4.00.

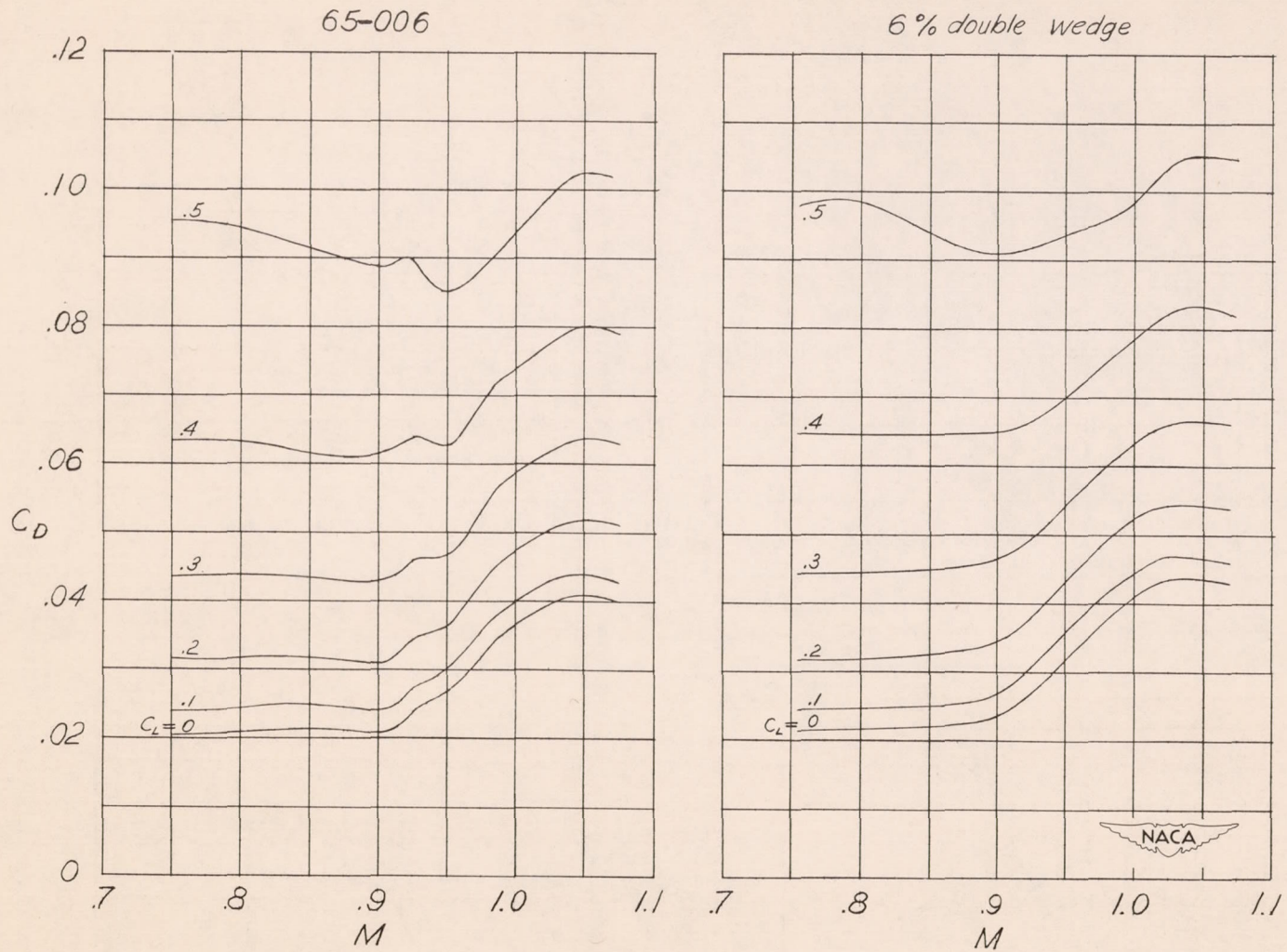
Figure 6.- Concluded.





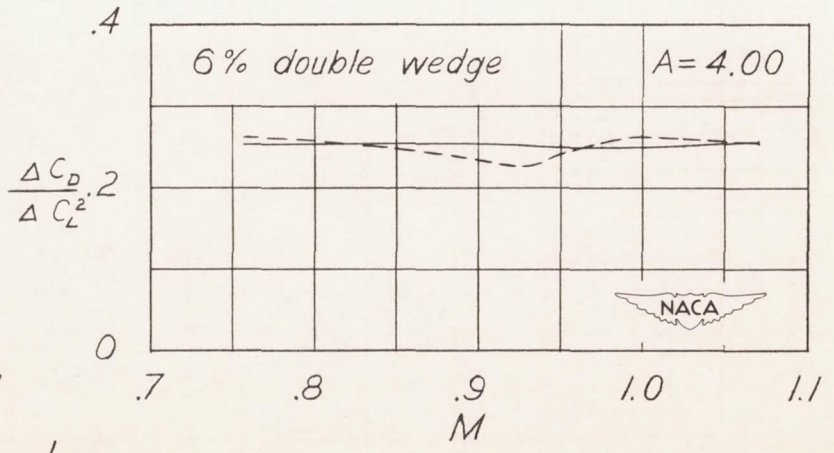
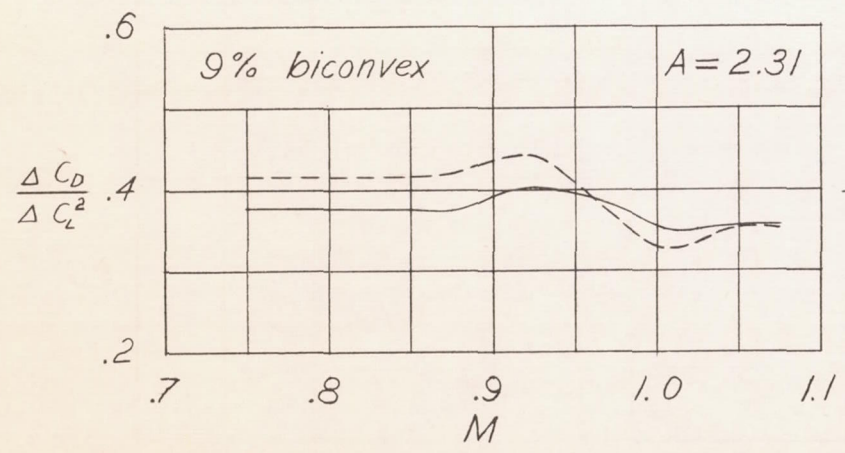
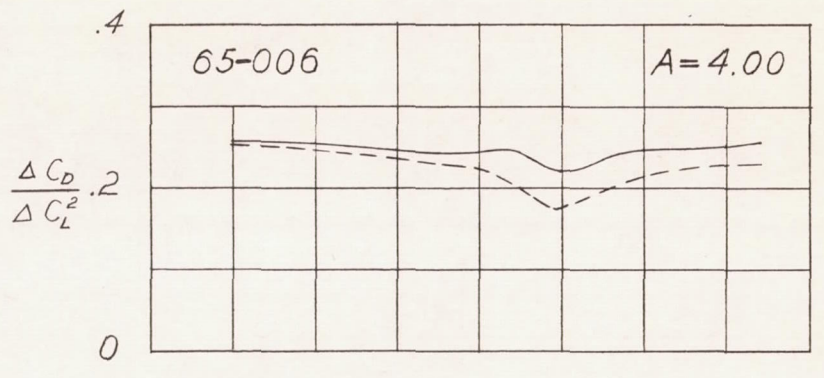
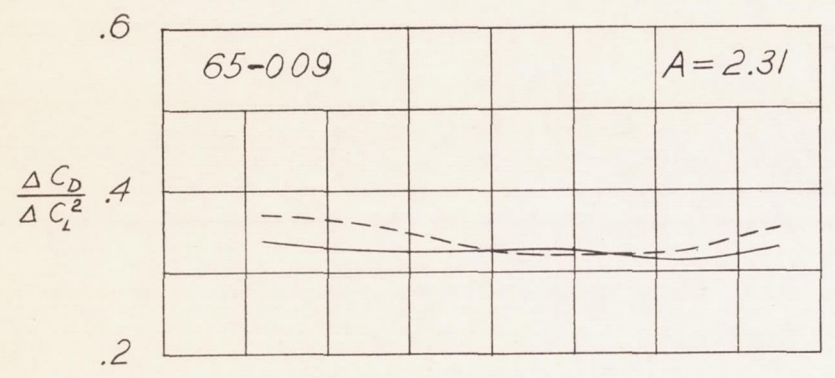
(a) Wing aspect ratio, 2.31.

Figure 8.- Variation of drag coefficient with Mach number at constant lift coefficient for wing-fuselage configurations.



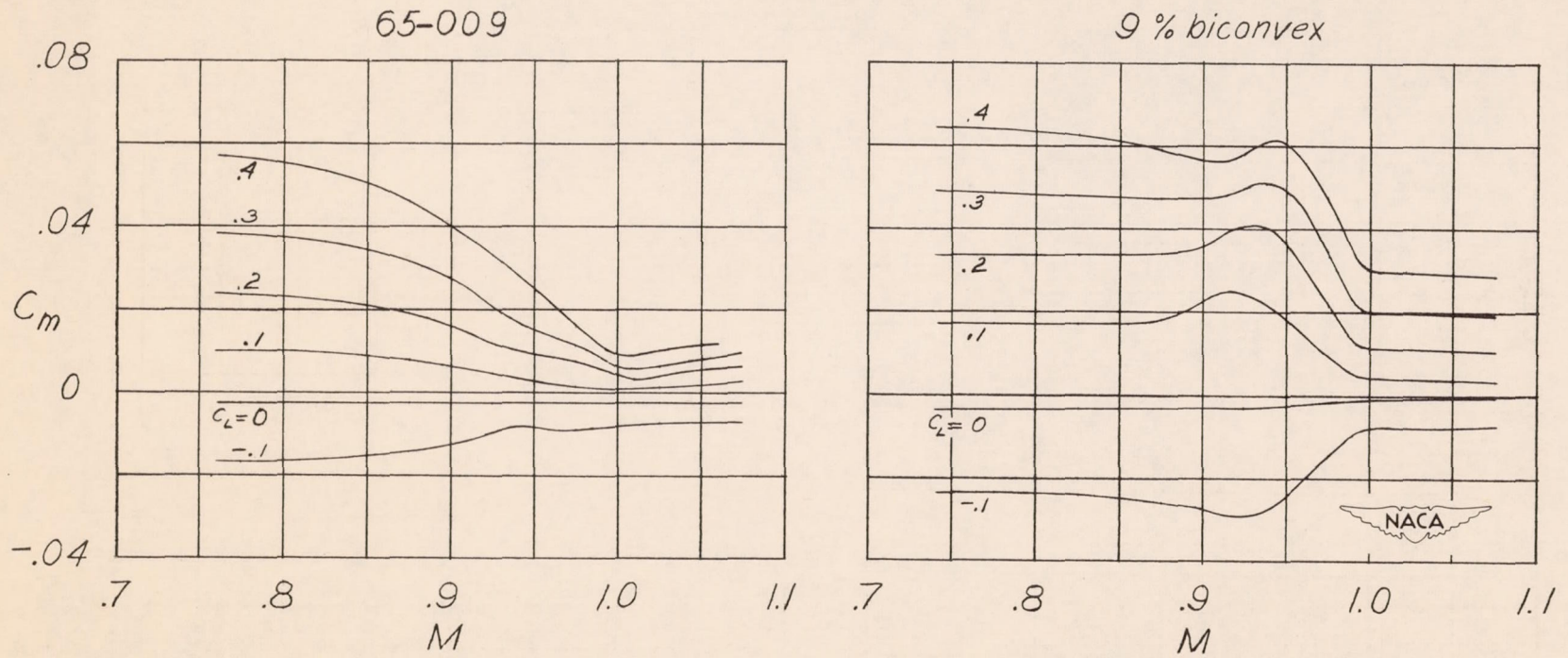
(b) Wing aspect ratio, 4.00.

Figure 8.- Concluded.



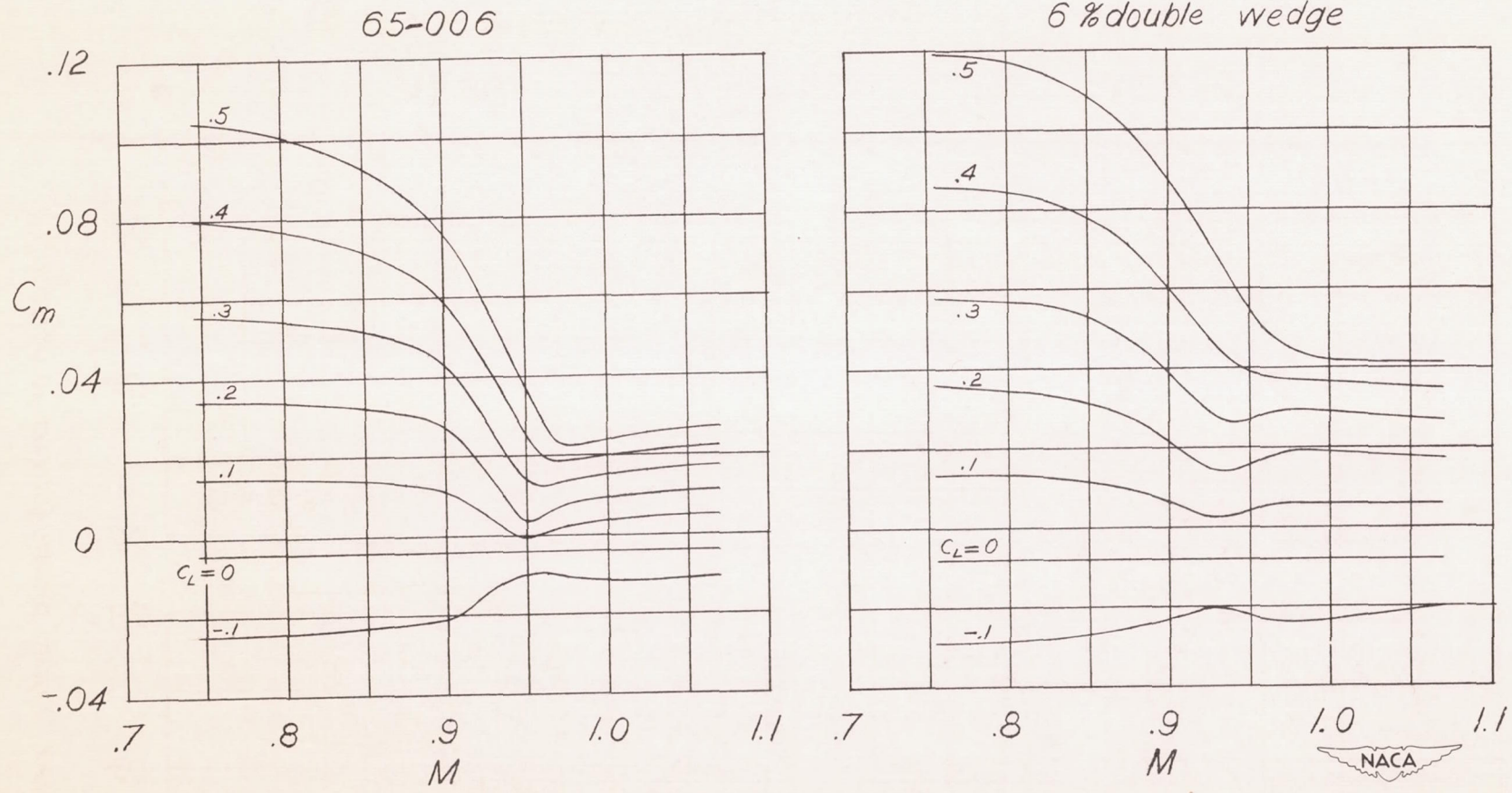
$$- - - - - \frac{1}{57.3 \frac{dC_L}{d\alpha}}$$

Figure 9.- Effect of Mach number on the factor $\Delta C_D / \Delta C_L^2$. Reciprocal of lift-curve slope also shown.



(a) Wing aspect ratio, 2.31.

Figure 10.- Variation of pitching-moment coefficient with Mach number at constant lift coefficient for wing-fuselage models.



(b) Wing aspect ratio, 4.00.

Figure 10.- Concluded.

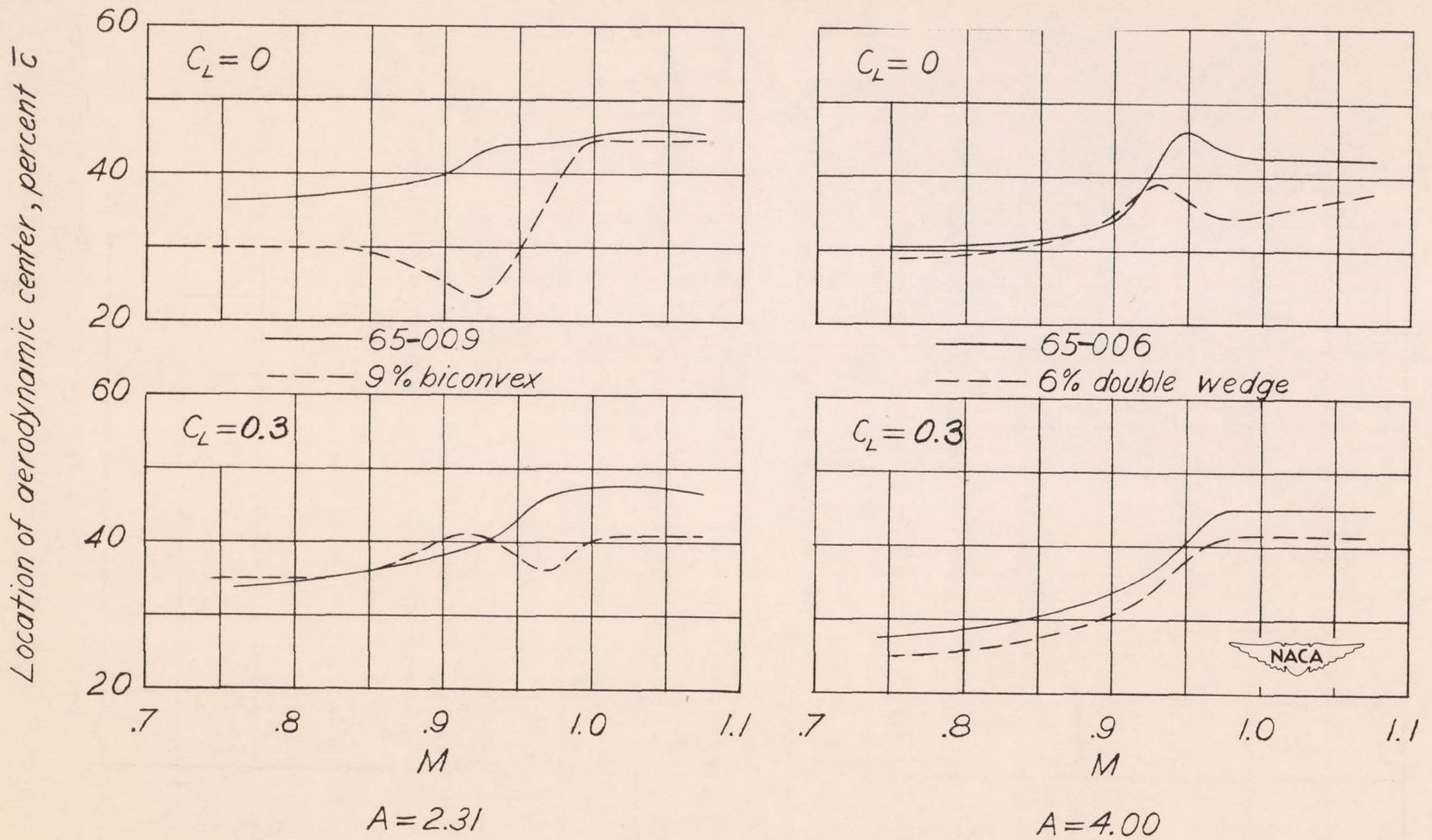


Figure 11.- Effect of Mach number on location of the aerodynamic center.